Thamboo, Julian, Zahra, Tatheer, & Asad, Mohammad
(2021)
Monotonic and cyclic compression characteristics of CFRP confined masonry columns.
Composite Structures, *272*, Article number: 114257.

https://doi.org/10.1016/j.compstruct.2021.114257

Monotonic and cyclic compression characteristics of CFRP confined masonry columns

Julian Thamboo[1], Tatheer Zahra[2], Mohammad Asad[2]

[1]Department of Civil Engineering, South Eastern University of Sri Lanka, 32360 Oluvil, Sri Lanka, jathamboo@seu.ac.lk

[2]School of Civil & Environmental Engineering, Queensland University of Technology, Brisbane, QLD 4000, Australia

Abstract

The lateral confinement of masonry columns using composites have shown to improve their strength and ductility. Although, several research studies were focused on investigating the monotonic compression behaviour of confined masonry columns in the past, their cyclic compression characteristics, which are necessary for seismic and dynamic analyses, are not well investigated. Thus, an attempt has been made to experimentally characterise the confined masonry columns under monotonic and cyclic axial compression in this research. In total, 36 masonry columns were built and tested under monotonic and cyclic compression. Out of 36 columns, twelve columns were unconfined and tested under monotonic compression, while the rest of the columns were confined with Carbon Fibre Reinforced Polymer (CFRP) laminates and tested under monotonic and cyclic compression. The experimental results are presented in terms of observed failure modes, compressive strengths and stress-strain curves. Cyclic loading protocol was displayed to marginally reduce the compressive strength of CFRP confined masonry columns by 6% to 13% compared to the compressive strengths obtained through monotonic compression testing. The analytical models available to predict the monotonic stress-strain curves were used to predict the cyclic envelop stress-strain relationship of confined masonry columns. Finally, the best fit analytical model to predict the cyclic envelop compression behaviour of CFRP confined masonry columns has been proposed.

Keywords: Confined Masonry Column; CFRP; Monotonic compression; Cyclic compression; Stress-strain curve; Envelop curve

1 Introduction

Majority of the historical masonry structures around the world usually have adequate loadbearing capacity to resist and transfer gravity actions. However, masonry is vulnerable to earthquake, extreme wind, differential settlement and deterioration caused by adverse environmental effects due to weak tensile and ductile characteristics. The capacity of masonry columns is of prime concern as the column failure could create substantial distress to the entire structure. To address this issue, different strengthening techniques have been developed in the past to enhance the strength and deformation characteristics of masonry columns [1-4].

Confining of masonry columns with Fibre Reinforced Polymers (FRP) has shown to enhance the strength and deformation behaviour to resist the axial and lateral loads. Micelli et al. [5] and Masia and Shrive [6] were the initial research studies reported on the behaviour of FRP confined masonry columns. Subsequently, several other research studies were carried out on this topic with different types of FRPs in combination with various masonry assemblies [7-16]. These studies concluded that despite of the advantages of using FRPs for enhancing the strength of masonry columns; their drawbacks such as poor performance in elevated temperatures, incompatibility with masonry substrate and irreversibility cannot be ignored [17-20]. Nevertheless, several alternative application techniques are in development to overcome the irreversibility and incompatibility issues of FRPs with masonry substrate [21-22].

Moreover, the strength and stress-strain characteristics of FRP confined masonry under compression are essential for the design and analysis purposes. Through extensive experimental studies, several analytical models were developed to predict the strength of masonry confined with FRP in the past [23-26]. However only few analytical models were proposed for the monotonic stress-strain characteristics of masonry columns confined by FRP [27-28]. Most of these analytical models were primarily derived from similar studies on FRP confined concrete columns in the past [29-31]. However, the stress-strain characteristics of FRP confined masonry columns under cyclic compression are also important for the seismic and dynamic analyses. Since the masonry is commonly considered to possess zero tensile strength, the cyclic compression loading characteristics are needed for hysteresis analyses of masonry elements/structures, however these have not been well explored in the past.

In contrast, the strength and deformation behaviour of FRP confined concrete and reinforced concrete columns under cyclic compression are extensively investigated [32-34]. Several analytical models were also developed to predict the cyclic compression stress-strain behaviour for FRP confined concrete columns [35-38]. It can be hypothesised that the behaviour of FRP confined masonry columns would be different to FRP confined concrete columns due to anisotropic nature of masonry and different compatibility of masonry substrate with FRP as compared to concrete. Also, limited studies on the cyclic behaviour of unconfined/unreinforced masonry under axial compression [39-44] have suggested that the cyclic characteristics of masonry are different to the monotonically tested masonry. Consequently, it can be stated that the compressive response of FRP confined masonry under cyclic loading would be different to monotonic compression, as the cyclic loading normally induces progressive damage and reduces the stiffness (resembling low-cycle fatigue evaluation), which leads to different load-displacement/stress-strain characteristics than that of monotonic loading protocol.

As the cyclic compression behaviour of FRP confined masonry columns is not well explored in the past, an experimental investigation has been implemented to study the monotonic and cyclic compression behaviour of FRP confined masonry columns. Subsequently, 36 masonry columns have been built and tested to investigate monotonic and cyclic compression behaviour. Carbon fibre reinforced polymer (CFRP) laminate was used to confine the masonry columns. Primarily, four different masonry column assemblies were examined to study the influence of confinement under monotonic and cyclic compression. The experimental results are presented and discussed in terms of strength and deformation characteristics of CFRP confined masonry columns. Further, the available analytical models to define the monotonic compressive behaviour of FRP confined concrete/masonry columns were used to verify the cyclic stress-strain envelop of the tested masonry columns in this research programme.

2 Experimental Programme

Different types of masonry assemblies can be found in historical and modern structures with various types of units and mortars. In general, they can be divided into four categories (1) high strength units with low strength mortar (2) low strength units with low strength mortar (3) moderately high strength mortar with high strength units and (4) relatively high strength mortar with low strength units. The mechanical properties of masonry made with these different unit and mortar combinations vary due to difference in the strength and deformation characteristics of constituents [45-49]. These four types of masonry assemblies were considered in this research by selecting different unit and mortar types to construct masonry columns to relate to these assemblies. In the following sub-sections, the selection and testing of constitutive materials (i.e. units, mortar and CFRP), construction of masonry columns, application process of CFRP and testing methods are outlined.

2.1 Material characterisation

Two types of clay bricks were selected to represent the low and high strength brick masonry assemblies. The selected bricks are referred as B1 and B2 in this paper. The dimensions of the B1 and B2 bricks are 200 mm × 95 mm × 65 mm (length × width × height) and 210 mm × 100 mm × 60 mm, respectively. Six bricks were randomly selected from each type and their compressive strengths were obtained as per BS EN 772-1 [50]. The mean compressive strengths of the B1 and B2 bricks were 4.2 MPa (COV = 10.2 %) and 14.3 MPa (COV = 6.7 %), respectively. Accordingly, the B1 and B2 bricks were considered as the low and high strength bricks, respectively in this research. In order to determine the elastic moduli of the bricks, clip gauge as shown in Fig. 1(a) was attached on the brick face and the axial deformation were captured. The mean elastic moduli of the B1 and B2 bricks were 3238 MPa (COV = 13.4 %) and 10,456 MPa (COV = 9.7 %), respectively.

In addition, two types of mortars were prepared to assemble the masonry columns using natural hydraulic lime (NHL) and Ordinary Portland cement (CM). These two types of mortars were selected to represent low and high mortar strength characteristics found in masonry assemblies. The mix proportions of both mortars were prepared with the binder to sand ratio of 1:3 by volume. Mortar cylinders of 200 mm × 100 mm (height × diameter) were prepared as per ASTM C780 - 18a [51] during the construction of columns and tested after 28 days to determine the compressive strengths under displacement control mode. The compression testing of mortar cylinder is shown in Fig. 1(b). Three extensometers were fixed to the mortar cylinders to measure the axial deformation and to determine the elastic moduli of the mortars. The mean compressive strength of the NHL and CM mortars were 1.89 MPa (COV = 11.3%) and 13.6 MPa (COV = 8.7%), respectively. The mean elastic moduli of the NHL and CM mortars were 1233 MPa (COV = 10.5 %) and 8764 MPa (COV = 8.7 %), respectively.

Unidirectional CFRP laminate was used to confine the masonry columns and its tensile strength was determined according to ACI 440.2R-08 [52] as shown in Fig. 1(c). Three CFRP laminate coupons were prepared and tested under uniaxial tensile loading. 20 mm strain gauges were pasted on either side (in the middle) of the CFRP coupons, and the tensile strain was measured under axial tensile loading. Displacement loading rate of 2 mm/min was assigned in the tensile testing of CFRP coupons. The measured mean tensile strength, elastic modulus and rupture strain of the CFRP were of 1465 MPa (COV = 6.5 %), 71 GPa (COV = 14.4 %), and 0.021 (COV = 10.6 %), respectively.

(a) (b) (c)

Fig 1. Testing of constituents (a) brick, (b) mortar and (c) CFRP.

2.2 Construction of masonry columns

In total, 36 masonry columns were constructed and tested under monotonic and cyclic compression with four different combinations of brick to mortar assemblies. Out of these, twelve columns were unconfined and tested under monotonic compression. The remaining columns were confined with CFRP and tested under monotonic and cyclic compression. Three masonry columns were constructed for each brick to mortar assembly and loading protocol. The complete test scheme and the geometries of the constructed masonry columns are given in Table 1. The nomenclature adopted to denote each tested column configuration consists of four parts, where the first set of letters refer to the type of brick used (B1 or B2), the second letter implies the confinement method (U-unconfined and C-CFRP confined) and the third set of letters denotes the type of mortar used (NHL and CM) and the fourth letter designates the type of applied loading (monotonic-M and cyclic-C). For an example, B2-C-CM-C refers to the masonry column constructed of B2 bricks with CM mortar and confined by CFRP sheets and tested under cyclic protocol.

The masonry columns were constructed with 10 mm mortar joints. After 14 days of the construction of the columns, the CFRP laminates were applied to the columns. As recommended in the CNR-DT 200 [27], the edges of the constructed masonry columns were ground to create a 20 mm radius fillet. Before wrapping the CFRP sheets around the columns, the column surfaces were scrubbed with wire brush to remove any loose particles and then an epoxy primer coat was applied. Then, the CFRP sheets were manually wrapped laterally around the columns as shown in Fig. 2 and pressed by metal rollers to remove any entrapped air. An overlapping of 150 mm was adopted to ensure adequate bonding and prevent lapping failure during the testing. Thereafter, another epoxy coat was applied on the finished surface of the CFRP smeared column. All the masonry columns were air cured for 28 days preceding to testing in the laboratory, where the temperature (28 ºC ± 2 ºC) and humidity (55 % - 70 %) remained quite steady.

Table 1: Test scheme and geometries of the masonry columns

Specimen Notation	Unit Type	Confinement	Mortar type	Testing protocol	Column Dimension Length×Width×Height/ (mm)	Number of samples tested
B1-U-NHL-M	B1	-	NHL	Monotonic	515×200×200	3
B1-C-NHL-M		CFRP		Monotonic		3
B1-C-NHL-C		CFRP		Cyclic		3
B1-U-CM-M		-	CM	Monotonic	515×200×200	3
B1-C-CM-M		CFRP		Monotonic		3
B1-C-CM-C		CFRP		Cyclic		3
B2-U-NHL-M	B2	-	NHL	Monotonic	480×210×210	3
B2-C-NHL-M		CFRP		Monotonic		3
B2-C-NHL-C		CFRP		Cyclic		3
B2-U-CM-M		-	CM	Monotonic	480×210×210	3
B2-C-CM-M		CFRP		Monotonic		3
B2-C-CM-C		CFRP		Cyclic		3

(a) (b)

Fig 2. Application of CFRP sheets to the masonry columns (a) Epoxy coating and (b) wrapping of CFRP sheets.

2.3 Instrumentation and Testing

The compression testing of the masonry columns was carried out using a 1000 kN capacity servo-controlled universal testing machine (UTM). The columns were aligned in the centre of the loading platens of the UTM to minimise any eccentricity. The loading platen of the UTM was hinged to the spherical seating to avoid loading misalignment. In order to reduce the platen restraint between the masonry and steel loading platen, 5 mm plywood capping was inserted at the top and bottom of the masonry columns. The testing arrangement is shown in Fig. 3. The monotonic loading was applied using a displacement-controlled loading rate at 0.5 mm/min. Due to the limitations of measuring displacements at a time in the datalogger, only two displacement transducers were fixed in the vertical position on two opposite faces (one per each face) to capture the vertical deformation of the columns. However, as mentioned, care was taken to minimise any eccentricity in the axial compression loading and the data from the two displacement transducers was continuously monitored to determine the vertical shortening of the columns. Also, the derived axial stress-strain curves (presented in sections 3.2 and 3.3) using these measurements showed no abnormalities, which justifies the adequacy of using only two transducers for measuring the vertical displacements. Another, two displacement transducers (one per each face) were laterally fixed in horizontal direction on the same faces to capture the lateral dilation of the columns under compression. In addition, two 20 mm strain gauges were pasted (to the opposite faces) at the middle of the columns on the CFRP sheets to measure the lateral tensile strain development under axial compression loading. The loads and displacements were recorded using a datalogger.

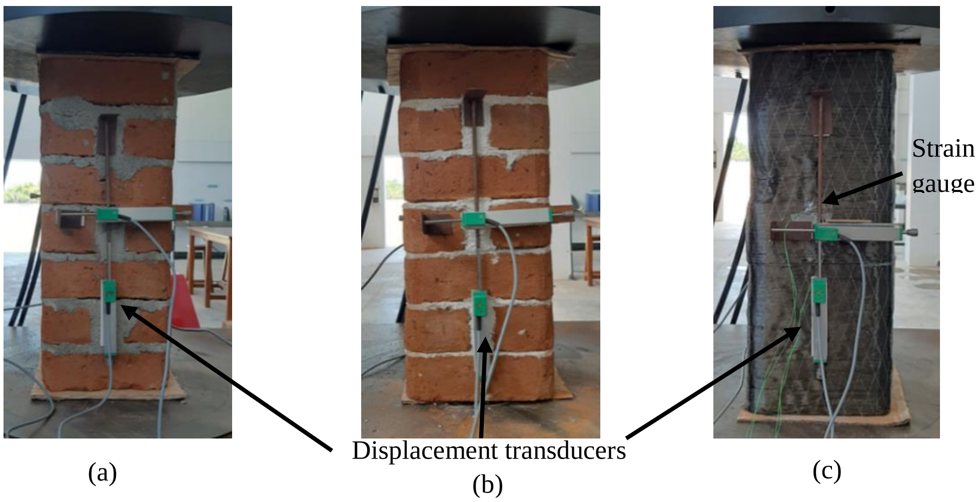

Fig 3. Testing of masonry columns (a) CM mortared columns (b) NHL mortared column and (c) CFRP confined columns.

The cyclic loading protocol was defined from the axial load-displacement characteristics, which were obtained from the monotonic testing of the columns. A similar cyclic loading protocol was employed earlier by the first author to determine the cyclic compression behaviour of unreinforced masonry [44, 53-54] and the same methodology was extended to this experimental programme as well. A schematic cyclic loading protocol is presented in Fig. 4. The critical points in the axial load-deformation curves, such as elastic range, hardening range and peak points were characterised in the monotonic load-displacement response and was used in the cyclic loading protocol. The elastic limit point was taken as the one-third of the peak load measured in the monotonic load-displacement response. Whereas, the hardening limit point was taken as 0.8 times the peak load in the pre-peak region. Subsequently, cyclic loading steps were increased step by step in each limit range and at least two steps were assigned for each range to capture the complete response of the columns under cyclic compression. Each step was repeated twice to stabilise the readings as conventionally carried out in the cyclic loading protocols [42, 55]. The loading and unloading rates in the cyclic testing protocol were maintained at 0.5 mm/min.

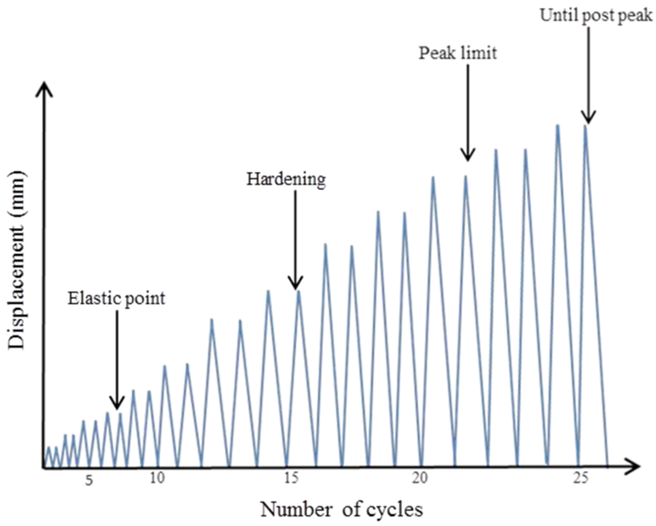

Fig 4. Schematic diagram of cyclic testing protocol.

3 Results and Discussion

The testing results of the unconfined and confined masonry columns are presented in terms of failure patterns, compressive resistance and axial stress-strain characteristics in the following sub-sections.

3.1 Failure patterns

The failure modes of the unconfined and CFRP confined masonry columns under compression loading are shown in Fig 5. The failure patterns of the unconfined masonry columns were characterised by vertical parallel cracks developed at the brick to mortar joints and developed throughout the height of the column until failure occurred as shown in Fig 5(a) and 5(b). This phenomenon of failure in unconfined masonry is well understood, that the incompatibility between the constitutive materials induces tensile cracks in the brick or mortar that depends on the relative deformation characteristics under axial compression [56-57]. Especially, when lower strength mortar was used in comparison to bricks (columns made with NHL mortar), the dilation of mortar under axial compression induces tensile cracks in the bricks, and vice versa also can happen. Whereas when the mortar is stronger than bricks (i.e. B1-U-CM column), the tensile cracks started in the mortar joints and propagated into the bricks.

The ultimate failure pattern of the CFRP confined masonry were characterised by complete crushing failure of masonry core or the rupture or delamination of CFRP, or sometimes combined phenomenon of masonry crushing and CFRP delamination. Since the masonry assembles were fully covered by the CFRP, the detail crack development in the masonry was not noted properly. However, inspection of the tested columns revealed that masonry cores were cracked as shown in Fig 5(e) and (f), nonetheless the CFRP wrapping held the cracked masonry without any collapse. During the initial stages of the loading, the delamination of CFRP from the masonry substrate was noted by progressive noises, which highlighted continuous internal debonding between CFRP and masonry as shown in Fig. 5(c) to 5(f).

Fig 5. Failure patterns of unconfined and CFRP confined masonry (a) Unconfined column with CM mortar (b) Unconfined column with NHL mortar (c) rupture of FRP and crushing of masonry (d) Delamination in CFRP confined column (e) Failure of CFRP confined CM column (f) Failure in CFRP confined NHL column.

3.2 Monotonic and Cyclic Behaviour

3.2.1 Unconfined columns under monotonic loading

The unconfined compressive strengths and the associated deformation properties measured in the unconfined masonry columns under monotonic compression loading are presented in Table 2. The COV of these parameters are given in the parentheses. The axial stress-strain curves obtained for the unconfined masonry columns under monotonic compression are given in Fig. 6. The peak strain matches to the peak stress point in the stress-strain curve. The elastic modulus was calculated using the one-third of the peak compression stress and the corresponding strain values. The Poisson's ratio was determined using the elastic strain and relevant lateral strain in the stress-strain curves.

It can be observed that the unconfined compressive strengths of B1 series columns are lesser than the similarly mortared B2 series columns. Obviously, the compressive strengths of the bricks dominated the compressive strengths of the unconfined columns. Further, the change in mortar type from NHL to CM has slightly improved the compressive strengths. In B1 series, an increase of 23.8 % and in B2 series an increase of 10.1% was observed. The efficiency ratios of the unconfined columns were computed by dividing the compressive strengths of the columns by the compressive strength of bricks. It can be noted that the efficiency ratios of the tested unconfined columns ranged between 0.41 to 0.52, whereas variation in the brick or mortar types do not greatly vary the efficiency of the masonry columns under compression.

The change in types of brick and mortar influenced the deformation characteristics of the unconfined columns, where the B2 series columns showed less deformation than the B1 series columns. The average stress-strain responses obtained in each combination of unconfined column testing results are plotted in Fig 6(e) for comparison. It can be noted that, in general the lower strength NHL mortared columns have shown relatively greater deformability than the higher strength CM mortared columns. The elastic moduli of the tested columns ranged between 217 MPa to 3698 MPa and the Poisson's ratios varied between 0.17 to 0.23. Thus, it can be stated that the mechanical properties of the bricks and mortar materials greatly influence the deformation behaviour of the masonry assembly. The ascending portions of the axial stress-strain curves of the unconfined columns are generally linear till nearly 70% - 80% of the peak stress, after which the nonlinear ascending branch initiated and followed up to the peak stress. The post-peak descending branches of curves are highly non-linear, where rapid degradation of stress was noted with slight increment in strain. The ultimate strain was measured corresponding to 85% of the peak stress in the post peak region.

Table 2. Mechanical properties of unconfined columns under monotonic loading.

Specimen	Compressive strength (MPa)	Efficiency ratio	Peak strain	Ultimate strain	Elastic modulus (MPa)	Poisson's ratio
B1-U-NHL-M	1.76 (18.0)	0.42	0.008 (16.8)	0.0075 (18.2)	217 (21.0)	0.23 (18.2)
B1-U-CM-M	2.18 (9.5)	0.52	0.003 (18.1)	0.0036 (13.2)	716 (18.0)	0.18 (14.0)
B2-U-NHL-M	5.69 (5.6)	0.41	0.0054 (7.3)	0.0055 (14.8)	1256 (15.1)	0.21 (15.6)
B2-U-CM-M	6.27 (4.6)	0.44	0.0015 (5.6)	0.0022 (13.9)	3698 (8.1)	0.17 (8.2)

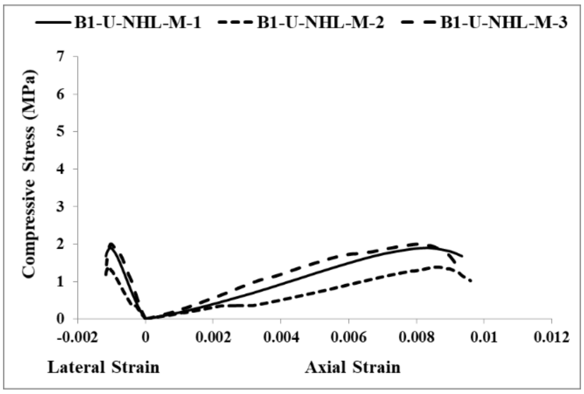

(a) B1-U-NHL-M

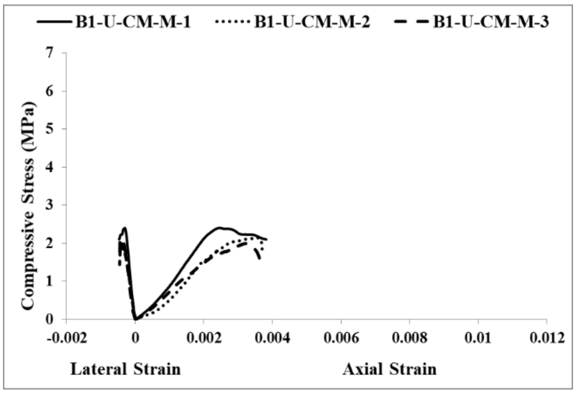

(a) B1-U-CM-M

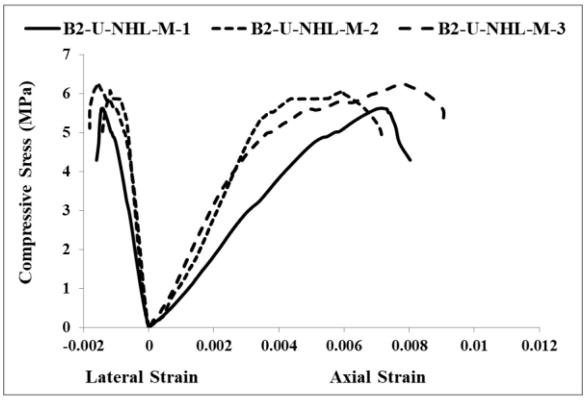

(c) B2-U-NHL-M

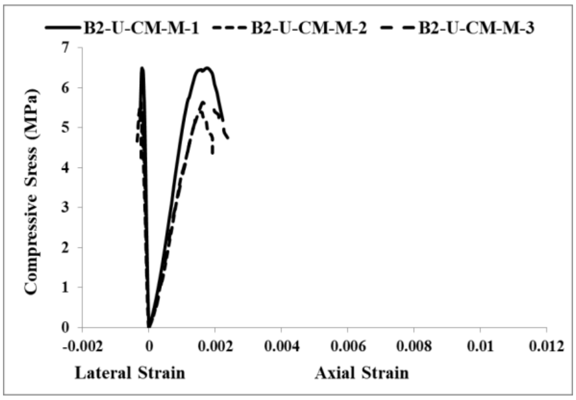

(d) B2-U-CM-M

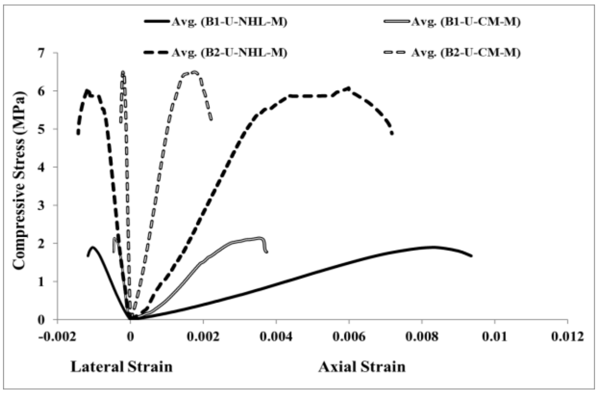

(e) Comparison of average curves

Fig 6. Monotonic compressive stress-strain behaviour of unconfined masonry columns.

3.2.2 Confined columns under monotonic loading

The compressive strengths and the associated deformation properties measured in the CFRP confined masonry columns under monotonic compression loading are presented in Table 3. Similar to the unconfined compressive strengths, the B2 series columns have shown higher compressive strengths than the B1 series columns. Also, the change in the mortar type, slightly changed the confined compressive strengths. The COV of compressive strengths are presented in the parentheses. The gain in compressive strength due to CFRP confinement was calculated by dividing the confined compressive strength by the corresponding unconfined compressive strengths. It can be noted that the strength gain varied between 154-301% for the tested combinations. Moreover, the ultimate strain was considered as the strain corresponds to 85% of the maximum stress reported in the stress-strain curves. Subsequently, the gain in ultimate strain, was computed by dividing the confined column ultimate strain by the unconfined column ultimate strain. The ultimate strain gain in the tested columns ranged between 280-500%. Therefore, it can be said that the CFRP confinement has shown to effectively enhance the axial strength and deformation characteristics of masonry columns.

Initial elastic moduli of the columns were also calculated from the initial linear portions of the curves, where the stress was taken as the one-third of the maximum stress measured in the linear portion, and the corresponding strain was used to compute the elastic modulus. The initial elastic moduli values show that they are in the similar range of unconfined columns, and the gain in initial modulus was marginal in the range of 10-13% for CM mortar in both B1 and B2 series. It could be stated that the unconfined and confined columns follow quite similar initial axial behaviour, until the dilation of the masonry core is enough to activate passive confinement by the CFRP laminates. However, the initial elastic modulus increment of B1-C-NHL-M columns was about 102% higher than the corresponding B1-U-NHL-M, this relatively higher increment could be attributed to the confinement provided to the columns made of weaker brick and mortar which restricted their usual large deformation. On the other hand, other three combinations of columns (B2 series) have shown a lesser increment (10%-41%) in the initial elastic modulus compared to their corresponding unstrengthened columns. This phenomenon of lower increment in the elastic modulus in these columns could be due to relatively stiffer nature of masonry assemblies, where the dilation of the masonry was prevented as compared to B1-NHL combination. Quite similar characteristics were reported in previous studies on the confined masonry columns under axial compression, where it was commonly believed that the confinement is more effective in lower strength masonry than the masonry assemblages made with stiffer constitutive materials [9, 22].

Hence, the behaviour of FRP confined masonry columns under compression depends on the deformation properties of masonry and the level of confinement provided by the CFRP laminates. The tensile strains on the surface of CFRP laminates at the failure are also presented in Table 3; one can note that the strain at failure was relatively lesser than the rupture strain of the CFRP (i.e. 0.021) which could be due to delamination of laminate occurred before it could rupture. The exploitation ratio was calculated by dividing the strain at failure by the rupture strain of CFRP that varied in the range of 0.61 to 0.29, thus indicating that the full potential of FRP was not utilised [9, 23, 25].

The axial stress-strain curves of the confined masonry columns under monotonic compression are given in Fig. 7. The axial stress-strain curves of the confined masonry columns followed a bilinear pattern typically, where initial linear portion is associated with the elastic behaviour of masonry core. With the cracking and dilation of masonry, the passive confinement effect was activated and caused nonlinearity. Thereafter, a relatively linear branch can be noted, which is associated with the rapid confinement of the masonry core until the failure caused by delamination of the CFRP laminate. The average stress-strain responses obtained in each combination of confined column monotonic loading are plotted in Fig 7(e) for comparison. As observed in the unconfined column results, the deformation characteristics are follow similar trend, where the NHL mortared columns with B1 bricks have shown higher deformity than the CM mortared columns with B2 bricks. Thus it implies, that the deformation characteristics of masonry constituents play a major role in the overall behaviour of confined masonry columns.

Table 3. Mechanical properties of confined columns under monotonic loading.

Specimen	Compressive strength (MPa)	Gain in strength (%)	Ultimate strain	Gain in ultimate strain (%)	Elastic modulus (MPa)	Gain in initial modulus (%)	Strain on FRP at failure
B1-C-NHL-M	5.33 (6.1)	+301	0.021 (13.9)	+280	440 (7.1)	+102	0.013 (18.9)
B1-C-CM-M	5.93 (8.3)	+272	0.019 (10.7)	+444	789 (14.8)	+10	0.011 (14.8)
B2-C-NHL-M	9.51 (7.6)	+172	0.018 (8.3)	+327	1773 (7.5)	+41	0.008 (19.9)
B2-C-CM-M	9.69 (11.9)	+154	0.011 (9.4)	+500	4195 (12.2)	+13	0.006 (20.0)

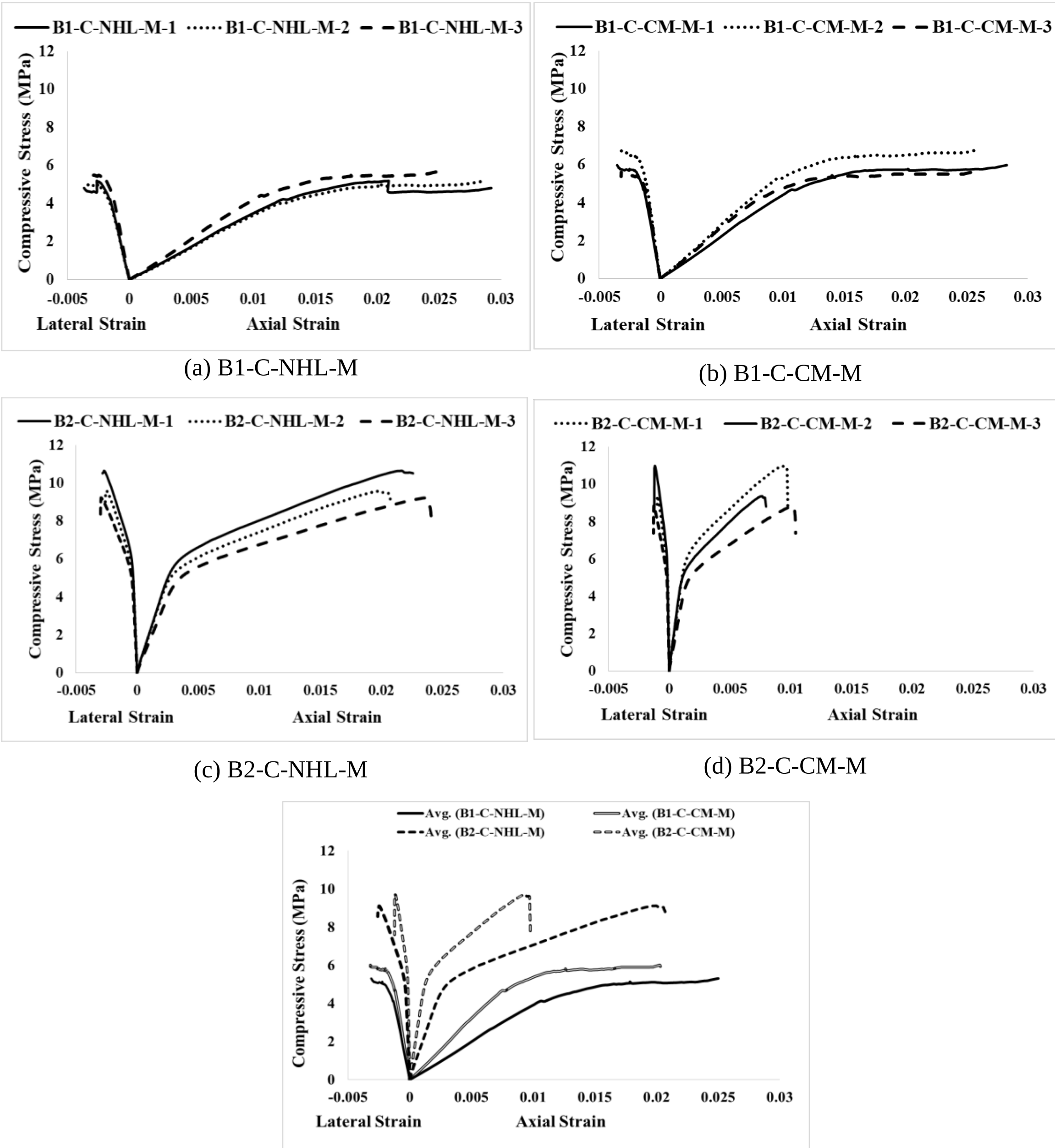

(a) B1-C-NHL-M

(b) B1-C-CM-M

(c) B2-C-NHL-M

(d) B2-C-CM-M

(e) Comparison of average curves

Fig 7. Monotonic compressive stress-strain behaviour of confined masonry columns.

3.2.3 Confined columns under cyclic loading

The cyclic confined compressive strengths and the associated deformation properties measured in the masonry columns under cyclic compression loading are presented in Table 4. The cyclic axial stress-strain curves of the confined masonry columns are given in Fig. 8. Out of three specimens tested in each combination, only one cyclic stress-strain curve is shown for each case, which is close to the average response, as showing all the curves in one graph will devoid comprehension. One can note from Table 4, that the variations of cyclic confined strengths follow similar trend as observed in the monotonic compressive strengths, where the B2 series columns have displayed higher compressive strengths than the B1 series columns. Also, the CM mortared columns have marginally higher compressive strength than the NHL mortared columns.

However, it can be observed that the cyclic confined compressive strengths are slightly lower than the corresponding monotonically loaded confined columns, where the reductions were observed in the range of 6-13% for the tested combinations. Also for comparison purposes, the average monotonic stress-strain curves presented in Fig 7(e), are plotted along with the corresponding cyclic plots obtained. The reduction in the compressive strength under cyclic testing was attributed by gradual build-up of non-reversible axial and lateral strains in the columns, with the increase in each step in the cyclic loading protocol. From the cyclic stress-strain responses presented in Fig. 8, the strength and stiffness deterioration at each step and cycle can be noticed, which describes that the progressive damage has occurred in each loading cycle in the confined columns.

Table 4. Mechanical properties of the confined columns under cyclic loading.

Specimen	Compressive strength (MPa)	Reduction in strength (%)	Ultimate strain	Elastic modulus (MPa)	Reduction in Elastic modulus (%)	Strain in FRP at failure
B1-C-NHL-C	4.97 (7.3)	-7	0.025 (8.8)	354 (14.1)	-19.5	0.014 (16.7)
B1-C-CM-C	5.43 (10.8)	-9	0.021 (9.4)	567 (15.0)	-28.2	0.012 (14.7)
B2-C-NHL-C	8.22 (6.3)	-13	0.020 (10.7)	1168 (15.6)	-34.1	0.009 (13.3)
B2-C-CM-C	9.11 (9.4)	-6	0.012 (9.2)	3388 (6.5)	-19.2	0.005 (18.9)

It can also be noted from Fig. 8, that in the second cycle of each step, the previously attained stress was not achieved, indicating the gradual damage occurs in each cycle and step, which ultimately led to the reduction in strength and stiffness of the FRP confined column. Similar phenomenon was noted in unreinforced masonry under cyclic compression, where the reduction in strength and stiffness were reported in the range of 15-25%, [44, 54]. However, the reductions observed in the FRP confined masonry members are comparatively less than the unreinforced/unconfined masonry. These results prove that the confinement technique improves the performance of masonry in cyclic compression loading.

The envelop curves for the cyclic stress-strain relationships were obtained by connecting the peak stress points in each step and as indicated in Fig. 8. Using the envelop curves, initial elastic moduli and ultimate strains were calculated as listed in Table 4. The magnitude of ultimate strains depicts that the axial deformations of the cyclic loaded confined masonry columns are slightly higher than the monotonically loaded columns. It could be due to a continuous damage of the masonry core in the cyclic loading; however, the confinement held the integrity of the column without collapse, which enabled them to undergo higher deformability than the monotonic loaded confined columns. The initial elastic moduli of the cyclic loaded confined columns vary in the range of 354 MPa to 3388 MPa, which are slightly less than the elastic modulus values obtained in the respective monotonic loaded columns. The reduction in the initial stiffness could have been initiated due to an early damage under the cyclic loading condition. Subsequently, it can be inferred that the monotonic and cyclic compressive characteristics of the CFRP confined masonry columns are not entirely the same due to different deformability characteristics. This demands the need of careful selection of the parameters for the design and analysis of the CFRP confined masonry columns under axial compression. The recorded tensile strain on the CFRP laminates at the failure in the cyclic loading were found comparable to their counterparts tested under monotonic loading.

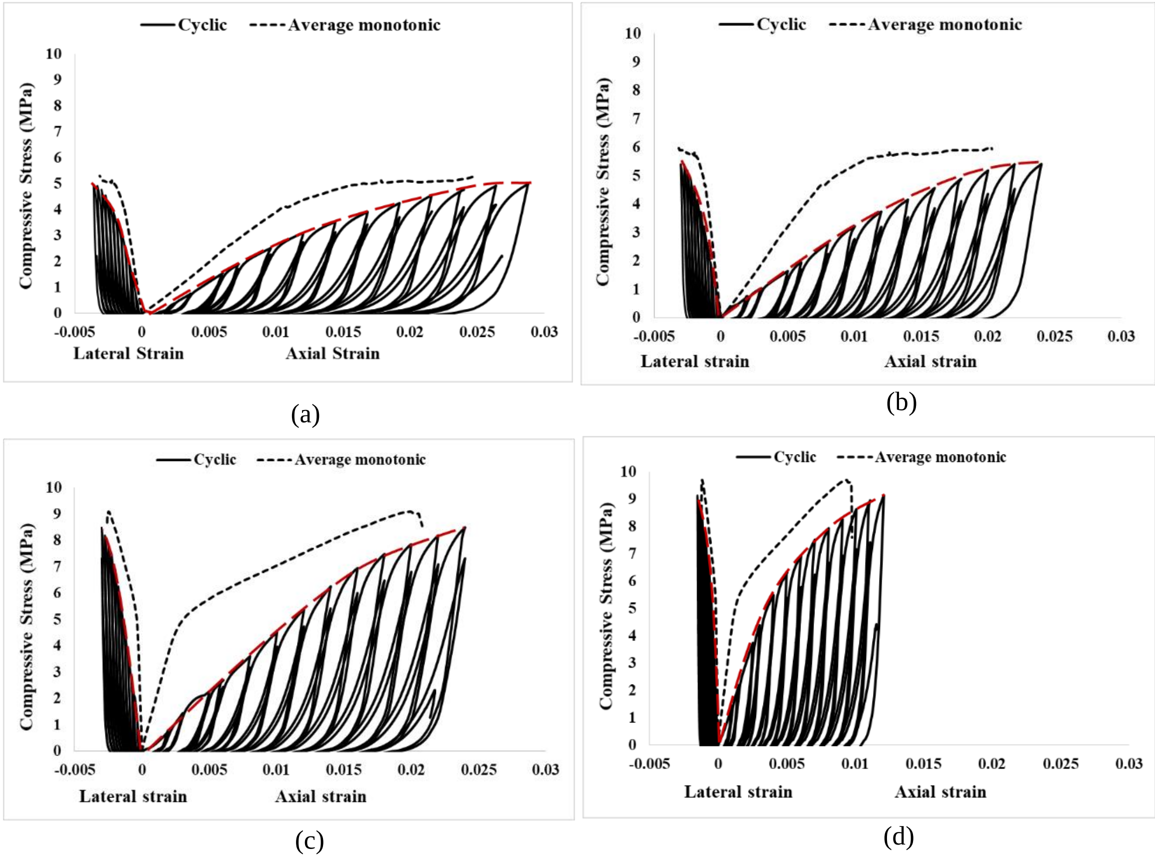

Fig 8. Cyclic compressive stress-strain behaviour of confined masonry columns (a) B1-C-NHL-C (b) B1-C-CM-C (c) B2-C-NHL-C (d) B2-C-CM-C

4 Verification of Analytical models

Most of the analytical studies on CFRP confined masonry were focused on determining the axial compressive strengths of different types of CFRP confined masonries in the past. Limited studies are available on analysing and developing axial stress-strain model of CFRP confined masonry from the experimental data [4]. To the authors' best knowledge no analytical stress-strain models are available in the literature for cyclically loaded confined masonry elements. Therefore, for comprehending the axial stress-strain characteristics of the CFRP confined masonry, the experimental monotonic and cyclic stress-strain data of this research were verified against the analytical stress-strain models given in the literature.

The available analytical stress-strain models can be categorised into two types: (1) Analysis oriented model (AOM) and (2) Design oriented model (DOM). The AOMs consider the interaction between the external confinement and internal core dilation, then incremental iterative computation procedures are used to resolve the force equilibrium and strain compatibility between the confined material and core. AOMs have the capability of accurately predicting the axial stress-strain behaviour of different confined masonry assemblies, given appropriate constitutive relationships of the individual materials are used. However, constitutive formulations defined in AOMs are based on several parameters which require extensive calibration. Whereas, the DOMs are based on the closed form expressions which can be directly derived from the experimental results. Since not many studies have been conducted on the monotonic and cyclic behaviour of CFRP confined masonry under compression, only the DOMs were considered in the analytical verification by the researchers.

Minafo et al. [58] compared the monotonic axial stress-strain predictions of two DOMs from the literature (1) CNR-DT 200 [27] and (2) Campione and Miraglia [30] with their experimental data of CFRP confined clay brick masonry. Recently, Sandoli and Calderoni [28] have proposed a DOM for CFRP confined tuff masonry which was modified from the model proposed by Lam and Tang [29] for CFRP confined concrete. The formulations used in these models are given in Table 5 with their associated parameters. The descriptions of the symbols are presented in the list of notations of this paper. Most of these analytical models have been derived primarily from the studies on monotonically tested CFRP confined concrete columns, whereas for cyclic behaviour of CFRP confined concrete in general, many studies are available [58-65]. These past studies on cyclic compression testing of CFRP confined concrete columns have revealed that the envelop curves of cyclic loaded columns are comparable to the corresponding monotonically loaded confined columns, and hence similar axial stress-strain formulations are proposed for monotonic and cyclic loaded confined concrete columns. Therefore, in this verification, the axial stress-strain models proposed for monotonically tested CFRP confined masonry (shown in Table 5) were considered for the verification of backbone envelop behaviour of cyclic loaded masonry columns.

For deriving the axial stress-strain response of the CFRP confined masonry columns, the axial compressive strengths should be predicted appropriately as defined in the formulations (see Table 5). One can note that the confined compressive strength relationships in the analytical models of CNR DT 200 [27] and Sandoli and Calderoni [28] are same. For calculating these parameters, the density of masonry (g_m) of the B1 and B2 series columns were taken as 1800 kg/m^3 and 2000 kg/m^3, respectively. The predicted confined compressive strengths are given in Table 6 with the percentage of difference between the experimental values. All analytical models are conservative, however the model given in Campione and Miraglia [30] under predicted the strength by an average of 50% for all cases, and therefore, not suitable for the development of stress-strain curves. Comparatively, the model predictions of CNR DT 200 [27] and Sandoli and Calderoni [28] were relatively closer to the experimental results, especially for B2 brick series which were considered for the stress-strain curves development.

The ultimate strain of the FRP confined columns under axial compression, were also predicted for the tested combinations as shown in Table 6. It can be noted that the models recommended in Campione and Miraglia [30] and CNR DT 200 [27] under predicted the ultimate strain values. While the ultimate strain formulations proposed in Sandoli and Calderoni [28] predicted relatively closer to the experimental values and can be used for the analysis as no other models are available. From these analyses, it can be inferred that the model of Sandoli and Calderoni [28] reasonably predicted both the confined compressive strength and the ultimate strain which was subsequently used to compare the stress-strain behaviour of the CFRP confined clay brick columns tested in this research.

Fig. 9 shows the average stress-strain responses of CFRP confined masonry columns for monotonic loading and average envelop curves for the cyclic loading with a comparison of predicted curves from the analytical model of Sandoli and Calderoni [28]. The average experimental responses were obtained for all tested combinations. It can be clearly noted from all four plots in Fig. 9, that the cyclic envelop stress-strain curves show lower stiffness than that of monotonic curves (as one could compare between the values of initial elastic modulus from Tables 3 and 4). Also, the ultimate strengths of cyclic loaded columns are slightly lower than their corresponding monotonically loaded column, however the reduction is marginal for B1 series columns (6%-13%) as presented in Table 4.

Also Iit can be observed that the analytical model predicted the axial stress-strain behaviour of the tested columns reasonably follow similar pattern despite the use of diverse constituents in the tested assemblies. In order to quantitatively compare the agreement between the experimental and analytical stress-strain curves, the regression analyses were carried out against the experimental and analytically predicted stress values (as the strain is an input for the analytical models) and the corresponding coefficient of determination (R^2) values were computed. The experimental and analytical predictions revealed that the R^2 varied between 0.79 to 0.95 for the monotonic and analytical data and ranged between 0.82 to 0.96 for the cyclic envelop and analytical data.

Table 5. Compressive stress-strain DOMs of CFRP confined masonry from the literature.

Reference	Stress-strain curve formulation	Confined compressive strength	Ultimate strain	Other parameters
Campione and Miraglia [30]	$f = f_{c0}\left[\frac{\beta\frac{\varepsilon}{\varepsilon_{c0}} + (1-\beta)\frac{\varepsilon}{\varepsilon_{c0}}}{\left(1+\left(\frac{\varepsilon}{\varepsilon_{c0}}\right)^{R}\right)^{1/R}}\right]$	$f_{cc} = f_{c0} + 2f_1'$	$\varepsilon_{ccu} = \varepsilon_{c0}\left[1 + \frac{\rho_f f_r}{\varepsilon_{c0}E_f(f_{c0} + k_e f_1)}\right]$	$\beta = \frac{E_h}{E_0}$, $E_h = \frac{f_{cc}-f_{c0}}{\varepsilon_{ccu}-\varepsilon_{c0}}$
Sandoli and Calderoni [28]	$f = \rho_2\frac{E_0^2}{100f_{cc}}\left[\frac{\varepsilon(2\varepsilon_{ccu}-1)}{\varepsilon_{ccu}} - \varepsilon^2\right]$ $f = (\alpha\varepsilon + \beta)f_{cc}$	$f_{cc} = f_{c0}\left[1 + k_1\left(\frac{f_1'}{f_{c0}}\right)^{\alpha_1}\right]$	$\varepsilon_{ccu} = \varepsilon_{c0} + 0.034\left(\frac{f_1'}{f_{c0}}\right)$	$\alpha_1 = 0.5$, $k_1 = \alpha_2\left(\frac{g_m}{1000}\right)^{\alpha_3}$ $\alpha_2 = \alpha_3 = 1$
CNR DT 200 [27]	$f = f_{c0}\left[a\frac{\varepsilon}{\varepsilon_{c0}} - \left(\frac{\varepsilon}{\varepsilon_{c0}}\right)^2\right]; 0 \le \frac{\varepsilon}{\varepsilon_{c0}} \le 1$ $f = f_{c0}\left[1 + b\frac{\varepsilon}{\varepsilon_{c0}}\right]; 0 \le \frac{\varepsilon}{\varepsilon_{c0}} \le \frac{\varepsilon_{ccu}}{\varepsilon_{c0}}$		$\varepsilon_{ccu} = 0.0035 + 0.015\left(\frac{f_1'}{f_{c0}}\right)^{0.5}$	$a = 1 + \gamma$, $b = \gamma - 1$ $\gamma = \frac{f_{c0} + E_h\varepsilon_{c0}}{f_{c0}}$

Table 6. Comparison of Experimental and analytical confined compressive strengths and ultimate strain.

	Confined Compressive Strength				Ultimate Strain					
Specimen	Campione and Miraglia [30]		Sandoli and Calderoni [28] & CNR DT 200 [27]		Campione and Miraglia [30]		Sandoli and Calderoni [28]		CNR DT 200 [27]	
	Predicted (MPa)	Difference (%)	Predicted (MPa)	Difference (%)	Predicted (mm/mm)	Difference (%)	Predicted (mm/mm)	Difference (%)	Predicted (mm/mm)	Difference (%)
B1-C-NHL-M	2.80	-90.3	3.28	-52.5	0.0012	-75.0	0.027	+22.3	0.013	-61.5
B1-C-CM-M	3.23	-83.5	4.26	-29.2	0.009	-77.7	0.019	+15.8	0.011	-45.5
B2-C-NHL-M	6.77	-40.4	8.38	-13.5	0.008	-125.0	0.012	-50.0	0.010	-80.0
B2-C-CM-M	7.20	-34.5	9.62	-7.0	0.008	-37.5	0.008	-37.5	0.009	-22.2
B1-C-NHL-C	2.80	-77.5	3.28	-51.5	0.0012	-108.3	0.028	+10.8	0.014	-78.6
B1-C-CM-C	3.23	-68.1	4.26	-68.1	0.010	-110.0	0.021	0	0.012	-75.0
B2-C-NHL-C	6.77	-21.4	8.38	+1.9	0.009	-122.2	0.014	-42.9	0.012	-66.7
B2-C-CM-C	7.20	-26.5	9.62	+5.3	0.008	-50.0	0.009	-33.3	0.010	-20.2
Average of absolute difference		50.7%		28.6%		86.2%		24.5%		56.2%

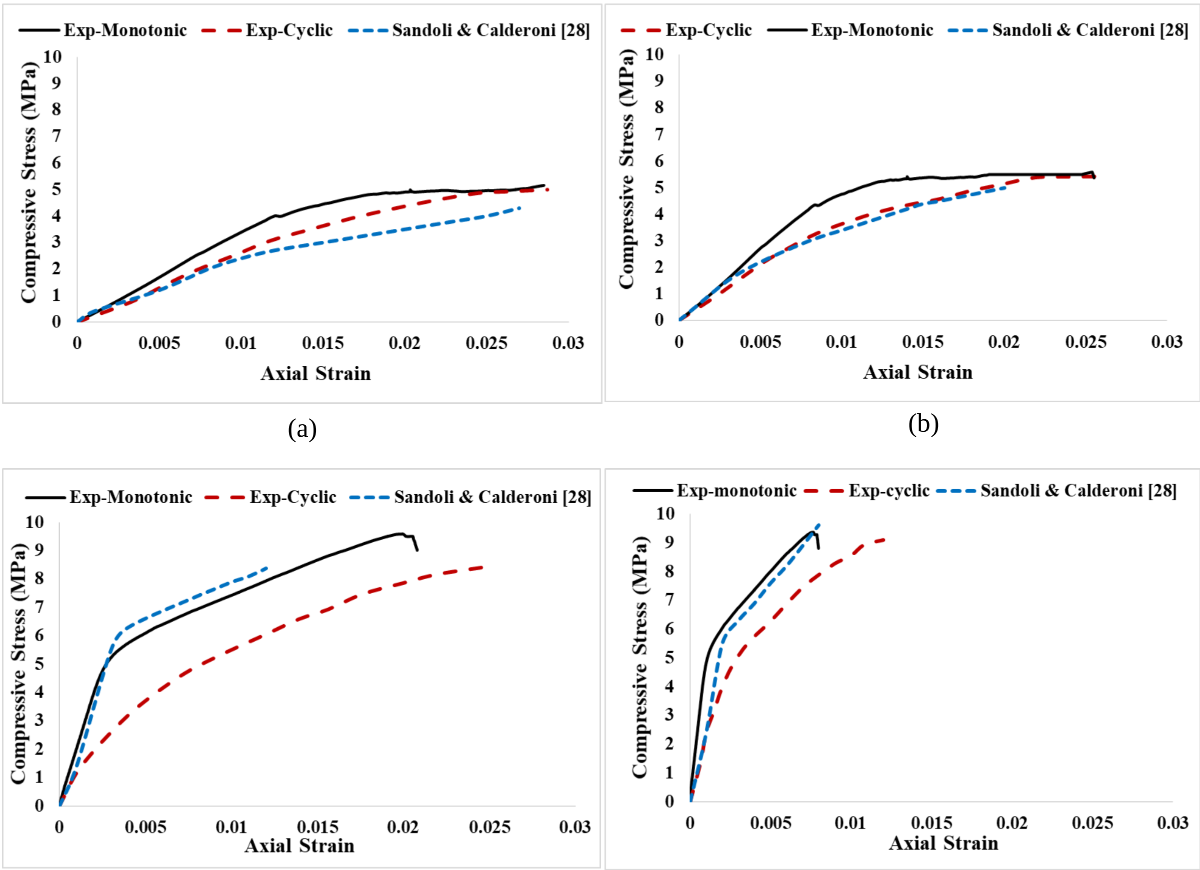

(a) (b) (c) (d)

Fig 9. Comparison of experimental and analytical stress-strain curves of CFRP confined masonry columns (a) B1-C-NHL (b) B1-C-CM (c) B2-C-NHL (d) B2-C-CM.

This concludes that the analytical formulations proposed by Sandoli and Calderoni [28] for CFRP confined tuff masonry are reasonability applicable to the CFRP confined clay brick masonry. Further verifications are necessary in the future to extend the understanding of various parameters such as CFRP application method (discontinuous application), shape of the columns (e.g. circle, rectangular, polygonal), and column aspect ratio, which can influence the axial stress-strain behaviour of CFRP confined columns under monotonic and cyclic loadings.

5 Summary and Conclusions

In this research, a detailed investigation on the monotonic and cyclic compression behaviour of CFRP confined clay brick masonry columns has been carried out. Mainly, four types of masonry column assemblies were constructed with two different types of clay bricks and mortars, which are commonly found in the masonry structures. In total, 36 masonry columns were tested in this research comprising of twelve unconfined and twenty-four CFRP confined columns. Out of twenty-four CFRP confined columns, twelve were tested under monotonic compression and the remaining were tested under cyclic compression. The experimental outcomes are presented in terms of failure modes, confined compressive strengths, and axial stress-strain responses for the monotonic and cyclic loadings. The experimental stress-strain data were also used to verify the application of the available analytical models proposed in the literature. Consequently, the following conclusions have emerged from the experimental and analytical verification.

- The axial compression behaviour of the confined and unconfined masonry columns is influenced by the masonry constitutive materials as revealed by the failure mode, strength and deformation characteristics of the four types of masonry column assemblies considered in this experimental investigation.
- The strength and deformation characteristics of monotonic and cyclic loaded CFRP confined masonry columns are different. Slight reduction in confined compressive strength (6-13%) and marginally higher deformation characteristics were obtained in cyclic loaded confined columns than the monotonic confined columns. The recorded elastic moduli and ultimate strains also justify the differences between the two loading protocols.
- Three analytical models considered for validating the experimental data were conservative in predicting the confined compressive strength and ultimate strain values. However, the formulations proposed by Sandoli and Calderoni [28] conservatively predicted the confined compressive strengths, ultimate strains, and the axial stress-strain behaviour of the CFRP confined clay brick masonry columns tested.

It should be highlighted that this experimental data is useful in understanding the monotonic and cyclic behaviour of CFRP confined masonry columns made with four different combinations of weak and strong bricks and mortars. However, the influence of other parameters such as discontinuous CFRP wrapping, shape of the columns, and the column aspect ratios to the cyclic compression behaviour of the CFRP confined masonry columns require investigation. The proposed formulations in the literature can be improved to predict the axial stress-strain behaviour of confined columns, using wider experimental data incorporating the effect of various influencing parameters.

6 CRediT authorship contribution statement

Julian Thamboo: Conceptualization, Funding acquisition, Formal analysis, Data Curation, Writing - Original Draft. **Tatheer Zahra**: Data Curation, Writing - review & editing. **Mohammad Asad**: Formal analysis, Data Curation.

7 Conflict of interest

The authors declare there are no conflicts of interest in this research.

8 Acknowledgements

The authors acknowledge the South Eastern University of Sri Lanka for the financial support to this project (under the research grant of SEU/ASA/RG/2019/02). The technical assistance provided by Mr Mohamed Jiffry, Mr Mohamed Farhan and Mr Mohamed Imthyas are greatly appreciated.

List of notations

f	Compressive stress
f_{c0}	Unconfined compressive strength
β	A parameter defined in Campione and Miraglia [25]
ε	Compressive strain
ε_{co}	Peak strain of unconfined masonry
R	A parameter defined in Campione and Miraglia [25]
f_{cc}	Confined compressive strength
f'	Effective confinement stress
ε_{ccu}	Ultimate strain in confined masonry
ρ_f	FRP strengthened ratio
f_r	Stress in FRP
E_f	Elastic modulus of FRP
k_e	Shape factor of the effective confinement stress
E_h	Modulus of the initial linear branch of confined stress-strain curve
E_0	Elastic modulus of unconfined masonry
α,β	Parameters defined in Sandoli and Calderoni [23]
$\alpha_1, \alpha_2, \alpha_3$	Parameters defined in Sandoli and Calderoni [23]/ CNR DT 200 [22]
g_m	Density of masonry

a,b,γ Parameters defined in CNR DT 200 [22]

References

[1]. Shrive NG. The use of fibre reinforced polymers to improve seismic resistance of masonry. Constr. Build. Mater 2006; 20(4): 269-277.

[2]. Tumialan G, Micelli F, Nanni A. Strengthening of masonry structures with FRP composites. Struct Congress 2001: 21–3.

[3]. Kouris LAS, Triantafillou TC. State-of-the-art on strengthening of masonry structures with textile reinforced mortar (TRM). Constr. Build. Mater 2018; 188: 1221–1233.

[4]. Thamboo JA. Performance of masonry columns confined with composite under axial compression: A State-of the art review. Constr. Build. Mater. 2020; 121791.

[5]. Micelli F, De Lorenzis L, Galati N, La Tegola A. Confinement of natural block masonry columns using fibre reinforced polymer rebars and laminates. In: Proceedings of the 9th Canadian masonry symposium, Fredericton, Canada, 4–6 June 2001.

[6]. Masia MJ, Shrive NG, Tilleman D. Rehabilitation of masonry columns using carbon fibre wraps, Proceedings, 9th Canadian Masonry Symposium, Fredericton, New Brunswick. 2001. On CD 12 pp.

[7]. Alecci V, Bati SB, Ranocchiai G. Study of brickwork columns confined with CFRP composite. J. Compos. Constr 2009; 13: 179–187.

[8]. Aiello MA, Micelli F, Valente L. FRP-confinement of square masonry columns. J. Compos. Constr 2009; 13(2): 148–158.

[9]. Di Ludovico M, D'Ambra C, Prota A, Manfredi G. FRP confinement of tuff and clay brick columns: experimental study and assessment of analytical models. J. Compos. Constr 2010; 14(5): 583–96.

[10]. Faella C, Martinelli E, Paciello S, Camorani G, Aiello MA, Micelli F, Nigro E. Masonry columns confined by composite materials: experimental investigation. Composites: Part B Eng 2011; 42(4): 692–704.

[11]. Micelli F, Angiuli R, Corvaglia P, Aiello MA. Passive and SMA-activated confinement of circular masonry columns with basalt and glass fibers composites. Compos. B Eng 2014; 67: 348–62.

[12]. Witzany J, Cejka T, Zigler R. Failure mechanism of compressed short brick masonry columns confined with FRP strips. Constr. Build. Mater 2014; 63: 180188.

[13]. Micelli F, Ludovico MD, Balsamo A, Manfredi G. Mechanical behaviour of FRP-confined masonry by testing of full-scale columns. Mater. Struct 2014; 47: 2081–2100.

[14]. Micelli F, Ludovico MD, Balsamo A, Manfredi G. Mechanical behaviour of FRP-confined masonry by testing of full-scale columns. Mater. Struct 2014; 47: 2081–2100.

[15]. Minafo G, Monaco A, D'Anna J, La Mendola L. Compressive behaviour of eccentrically loaded slender masonry columns confined by FRP. Eng. Struct 2018; 172: 214–227.

[16]. D'Anna J, Amato G, Chen JF, Minafo G, La Mendola L. Effectiveness of BFRP confinement on the compressive behaviour of clay brick masonry cylinders. Compos. Struct 2020; 249: 112558.

[17]. Wang. J, Wan. C, Zeng. Q, Shen. L, Malik. MA, Yan. D. Effect of eccentricity on retrofitting efficiency of basalt textile reinforced concrete on partially damaged masonry columns. Compos Struct 2020 232: 111585.

[18]. Carozzi FG, Colombi P, Fava G, Poggi C. Mechanical and bond properties of FRP anchor spikes in concrete and masonry blocks. Compos Struct 2018; 183: 185–198.

[19]. D'Altri AM, Carloni C, Miranda S, Castellazzi G. Numerical modeling of FRP strips bonded to a masonry substrate. Compos Struct 2018; 200: 420–433.

[20]. Milani G, Fagone M, Rotunno T, Grande E, Bertolesi E. Development of an interface numerical model for C-FRPs applied on flat and curved masonry pillars. Compos Struct 2020; 241: 112074.

[21]. Cascardi A, Dell'Anna R, Micelli F, Lionetto F, Aiello MA, Maffezzoli A, Reversible techniques for FRP-confinement of masonry columns. Constr. Build. Mater. 2019; 225, 415–428.

[22]. P. Foraboschi, Effectiveness of novel methods to increase the FRP-masonry bond capacity, Compos. B Eng. 107 (2016) 214–232.

[23]. Krevaikas TD, Triantafillou TC. Masonry confinement with Fiber-Reinforced polymers. J. Compos. Constr 2005; 3-4: 128-135.

[24]. Corradi M, Grazini A, Borri A. Confinement of brick masonry columns with CFRP materials. Compos Sci Technol 2007; 67(9): 1772–83.

[25]. Faella C, Martinelli E, Paciello S, Camorani G, Aiello MA, Micelli F, Nigro E. Masonry columns confined by composite materials: design formulae. Compos. Part B Eng 2011; 42(4): 705–716

[26]. Lignola GP, Angiuli R, Prota A, Aiello MA. FRP confinement of masonry: analytical modeling. Mater Struct 2014; 47(12): 2101-15.

[27]. CNR-DT 200. Guide for the design and construction of externally bonded FRP systems for strengthening existing structures. Rome: Italian Council of Research (CNR); 2013. p. 1e144.

[28]. Sandoli A, Calderoni. B. Constitutive stress-strain law for FRP-confined tuff masonry. Mater Struct 2020; 53: 57.

[29]. Lam L, Teng JG. Design-oriented stress-strain model for FRP-confined concrete. Constr Build Mater 2003; 17(6-7): 471-489.

[30]. Campione G, Miraglia N. Strength and strain capacities of concrete compression members reinforced with FRP. Cem Concr Compos 2003; 25(1): 31–41.

[31]. Fanaradell T, Rousakis T and Karabinis A. Reinforced concrete columns of square and rectangular section, confined with FRP—Prediction of stress and strain at failure. Compos Part B Eng 2019; 174: 107046.

[32]. Ozbakkaloglu T, and Akin E. Behavior of FRP-confined normal- and high strength concrete under cyclic axial compression. J Compos Constr 2011; 16(4); 451– 463.

[33]. Li P, Sui L, Xing F, Zhou Y. Static and cyclic response of low-strength recycled aggregate concrete strengthened using fiber-reinforced polymer. Compos B Eng 2019; 160: 37–49.

[34]. Abbasnia R.; Hosseinpour F.; Rostamian, M, Ziaadiny H. Cyclic and monotonic behavior of FRP confined concrete rectangular prisms with different aspect ratios. Constr Build Mater 2013; 40: 118–125.

[35]. Shao Y, Zhu Z, Mirmiran A. Cyclic modeling of FRP-confined concrete with improved ductility. Cem Concr Res 2006; 28(10): 959-968.

[36]. Lam L, Teng JG. Stress-strain model for FRP-confined concrete under cyclic axial compression. Eng Struct 2009; 31: 308-321.

[37]. Rousakis TC, Karabinis AI. (2012). Adequately FRP confined reinforced concrete columns under axial compressive monotonic or cyclic loading. Mater Struct 2012; 45(7), 957–975.

[38]. Cascardi A, Micelli F, Aiello MA. Unified model for hollow columns externally confined by FRP. Eng Struct 2016; 111:119–30.

[39]. Ispir M, Ilki A. Behavior of historical unreinforced brick masonry walls under monotonic and cyclic compression. Arab J Sci Eng 2013; 38; 1993–2007.

[40]. Facconi L, Minelli F, Vecchio FJ. Predicting uniaxial cyclic compressive behavior of brick masonry: new analytical model. J Struct Eng 2018; 144: 4017213.

[41]. Segura J, Pela L, Roca P. Monotonic and cyclic testing of clay brick and lime mortar masonry in compression. Const Build Mater 2018; 193: 453-466.
[42]. Dhanasekar M, Shrive NG. Strength and deformation of confined and unconfined grouted concrete masonry. ACI Struct 2002; 99: 819–826.
[43]. Oliveira DV, Lourenço PB, Roca P. Cyclic behaviour of stone and brick masonry under uniaxial compressive loading. Mater Struct 2006; 39: 247– 257.
[44]. Thamboo JA, Dhanasekar M. Assessment of the characteristics of lime mortar bonded brickwork wallettes under monotonic and cyclic compression. Constr Build Mater 2020; 261: 120003.
[45]. Thamboo JA. Material characterisation of thin layer mortared clay masonry, Constr Build Mater. 230 (2020) 116932
[46]. Noor-E-Khuda S, Albermani F. Mechanical properties of clay masonry units: destructive and ultrasonic testing. Constr Build Mater 2019; 219: 111–120.
[47]. Thamboo JA, Dhanasekar M. Characterisation of thin layer polymer cement mortared concrete masonry bond. Constr Build Mater 2015; 82: 71–98.
[48]. Drougkas A, Roca P, Molins C. Numerical prediction of the behavior, strength and elasticity of masonry in compression. Eng Struct 2015; 90:15–28.
[49]. Zahra T, Dhanasekar M. Prediction of masonry compressive behaviour using a damage mechanics inspired modelling method. Constr Build Mater 2016; 109: 128–138.
[50]. BS EN 772-1:2011+A1:2015, Methods of test for masonry units. Determination of compressive strength, BSI.
[51]. ASTM C780-18a, Standard Test Method for Preconstruction and Construction Evaluation of Mortars for Plain and Reinforced Unit Masonry, ASTM International, West Conshohocken, PA, 2018.
[52]. ACI 440.2R-08. Guide for the design and construction of externally bonded FRP systems for strengthening concrete structures. ACI Committee 440, American Concrete Institute. Farmington Mills, MI; 2008. p. 76.
[53]. Thamboo JA, Dhanasekar M. Response of Brickwork Wallettes of Various Bonding Patterns under Monotonic and Cyclic Compression. In Proceedings of the 17th International Brick and Block Masonry Conference, Karkow, Poland, 5–8 July 2020.
[54]. Thamboo JA, Bandara J, Perera S, Navaratnam S, Poologanathan K, Corradi M. Experimental and Analytical Study of Masonry Subjected to Uniaxial Cyclic Compression. Materials 2020, 13, 4505.

[55]. Assa B, Dhanasekar M, Layered line element for the flexural analysis of cyclically loaded reinforced concrete beam-columns. Comput Struct 2000; 78(4): 517e527.

[56]. Zahra T, Dhanasekar M. A generalised damage model for masonry under compression. Int J Damage Mech 2016; 25: 629–660.

[57]. Thamboo JA, Dhanasekar M. Correlation between the performance of solid masonry prisms and wallettes under compression. J Build Eng 2019; 22: 429-438.

[58]. Minafo G, D'Anna J, Cucchiara C, Monaco A, La Mendola L. Analytical stress-strain law of FRP confined masonry in compression: literature review and design provisions. Compos Part B Eng 2017; 115: 160-169.

[59]. Abbasnia R, Hosseinpour F, Rostamian M, Ziaadiny H. Cyclic and monotonic behavior of FRP confined concrete rectangular prisms with different aspect ratios. Constr. Build. Mater 2013; 40: 118–125.

[60]. Wei YY, Wu YF. Unified stress–strain model of concrete for FRP-confined columns. Constr Build Mater 2012; 26 (1): 381–92.

[61]. Ozbakkaloglu T, Lim JC, Vincent T. FRP-confined concrete in circular sections: Review and assessment of stress–strain models. Eng Struct 2013; 49: 1068–1088.

[62]. Xu, JJ, Chen ZP, Xiao Y, Demartino C, Huang JH. Recycled Aggregate Concrete in FRP-confined columns: A review of experimental results. Compos Struct. 2017; 174: 277-291.

[63]. Li P, Wu YF. Stress-strain model of FRP confined concrete under cyclic loading. Compos Struct 2015; 134: 60–71.

[64]. M.M.T. Lakshani, T.K.G.K. Jayathilaka, J.A. Thamboo, Experimental investigation of the unconfined compressive strength characteristics of masonry mortars, J. Build. Eng. 32 (2020)101558.

[65]. T. Zahra, A. Jelvehpour, J.A. Thamboo, M. Dhanasekar, Interfacial transition zone modelling for characterisation of masonry under biaxial stresses, Constr. Build. Mater. 254 (2020) 118735.